NASA TECHNICAL MEMORANDUM

CASE FILE COPY

ANALYTICAL STUDY OF PRESSURE BALANCING IN GAS FILM SEALS

by John Zuk
Lewis Research Center
Cleveland, Ohio

ANALYTICAL STUDY OF PRESSURE BALANCING IN GAS FILM SEALS

by John Zuk

Lewis Research Center
National Aeronautics and Space Administration
Cleveland, Ohio

ABSTRACT

Proper pressure balancing of gas film seals requires knowledge of the pressure profile load factor (load factor) values for a given set of design conditions. In this study, the load factor is investigated for subsonic and choked flow conditions, laminar and turbulent flows, and various seal entrance conditions. Both parallel sealing surfaces and surfaces with small linear deformation were investigated. The load factor for subsonic flow depends strongly on pressure ratio; under choked flow conditions, however, the load factor is found to depend more strongly on film thickness and flow entrance conditions rather than pressure ratio. The importance of generating hydrodynamic forces to keep the seal balanced under severe and multipoint operation is also discussed.

NOMENCLATURE

A	area, in.^{2}
C	constant in friction factor - Reynolds number relation
C_L	velocity entrance loss coefficient
D	hydraulic diameter, 2h, in.
F	force, lbf
$\overline{F}$	pressure profile load factor (load factor)
$\overline{f}$	mean Fanning friction factor

h   film thickness (gap), in.

L   sealing face (dam) flow length, in.

M   Mach number

n   exponent in friction factor - Reynolds number relation

P   pressure, psia

ΔP sealed pressure differential, psi

Re   leakage flow Reynolds number

$T(x)$ linear tilt factor, $h_2^2(2h_1 + \alpha x)/2h_m(h_1 + \alpha x)^2$

u   mean velocity in x-direction, ft/sec

W   flow width, in.

x   coordinate in pressure gradient direction

α relative inclination angle of surfaces, m rad

β film thickness ratio, h_1/h_2

γ specific-heat ratio

η geometric balance ratio or modulus

μ absolute or dynamic viscosity, lbf-sec/in.^{2}

ρ density, lbf-sec^2/in.^{4}

Subscripts

0   sealed (reservoir) conditions

1   seal entrance

2   seal exit

3   ambient sump conditions

f   friction

i   inertia

hs   hydrostatic

sd   sealing face (dam)

n   net

m   mean

x   flow length location

INTRODUCTION

One of the prime objectives in gas film face seal design is to insure that the face loading is sufficiently low so high heat generation and high wear are prevented; however, contact or close clearance operation must be maintained at all operating conditions. Seal balance can be achieved, at least theoretically, by properly adjusting the secondary seal diameter (see Fig. 1). A common term used by seal designers is the geometric balance ratio or modulus. This modulus is defined as the ratio of the hydrostatic closing area to primary sealing face (dam) area and is used to determine the location of the secondary seal diameter. It is desirable to predict this location analytically.

Unfortunately, a gas film seal will usually only be "balanced" at one combination of operating conditions. This is the case because the pressure profile factor varies with the sealed gas pressure differential. The pressure profile load factor is defined as the ratio of sealed hydrostatic pressure closing force to sealing face pressure opening or separating force. The pressure profile factor is defined as the ratio of the net or average sealing (dam) face pressure to sealed pressure differential. From hereon, the pressure profile load factor will be referred to as the load factor. Both the load factor and geometric balance ratio have other names in the

literature (2) through (7) and sometimes defined in slightly different ways. Some of these names are listed in Table 1. Since the load factor can equal the geometric balance modulus at only one set of operating conditions, it is therefore impossible to completely balance an ordinary face seal for all situations. Engineering judgment must be employed to select the proper design. Furthermore, since gases are poor boundary lubricants, contacting gas film seals can generally only carry 1/4-lb to 3/4-lb per inch of circumference (1). Since the load factor strongly depends on the sealed pressure ratio for subsonic flow, a slight unbalance at large pressure differentials will greatly overload the seal.

Since advanced rotating machinery may require large pressure differential seals, the seal flow may be choked. Hence the emphasis of this study will be on how the load factor varies under choked flow conditions. Both parallel and linearly tilted surfaces and entrance effects will be considered.

ANALYSIS

Seal Force Balance Fundamentals

The importance of the load factor and the geometric balance ratio can be illustrated by considering a face seal force balance. The basic equation defining seal closing force is (see Fig. 2)

$$\text{NET CLOSING FORCE} = F_s \pm (F_f + F_I) + A_{HS}\, \Delta P - W \int_0^L P\, dx \qquad [1]$$

Design philosophies differ; however, a common pressure balancing practice for gas film seals is to select the spring force F_s, to overcome only the

frictional forces F_f and the inertial forces F_I. (The frictional forces are due to the secondary seals (e.g., O-rings, piston rings) and the antirotation lugs (e.g., torque pins) rubbing on the housing.)

A fundamental consideration in designing pressure balanced seals is the selection of the secondary seal diameter. This diameter determines the hydrostatic (pneumatic) closing force as illustrated in Fig. 1. By proper positioning of the secondary seal diameter, this closing force can be equal to the sealing dam pressure opening force or at least theoretically, any degree of seal face loading. The secondary seal diameter can be found from the geometric balance ratio, η where

$$\text{geometric balance ratio, } \eta = \frac{A_{HS}}{A_{SD}} \qquad [2]$$

Another important parameter is the pressure profile load factor, $\overline{F}$ which is defined as the pressure (pneumatic) opening force normalized to the sealed pressure differential force acting over the entire sealing dam (seal face) area or

$$\overline{F} = \frac{\text{Pressure opening force}}{\Delta P \, A_{SD}} \qquad [3]$$

Across a sealing dam

$$\text{Opening force} = W \int_0^L P \, dx$$

If the seal opening force is equated to the hydrostatic closing force

$$W \int_0^L P \, dx = \Delta P \, A_{HS} \qquad [4]$$

and substituting this condition into Eq. [3], the result is

$$\overline{F} = \frac{A_{HS}}{A_{SD}} = \eta \qquad [5]$$

When this situation exists, that is the load factor is equal to the geometric balance ratio, the seal is said to be <u>perfectly balanced</u>.

Once the load factor is known, the seal balance diameter can be simply calculated.

$$\text{Seal Balance Diameter} = \overline{F}(2R_2 - 2R_1) + 2R_1$$

(For a perfectly balanced seal, the seal balance diameter equals the secondary seal diameter.) For some cases the sealing dam opening force can be evaluated analytically and hence the load factor can be predicted analytically. Examples will now follow.

Incompressible Fluids

The simplest case that the load factor can be analytically predicted is for laminar, incompressible flow. For purposes of illustration, since many seal users are sealing liquids, this case will be developed. The pressure profile can be found from (7)

$$P = P_1 - \frac{\Delta P x}{L} T(x) \qquad [6]$$

Where $T(x) = \dfrac{h_2^2(2h_1 + \alpha x)}{2h_m\left(h_1 + \alpha x\right)^2}$, the tilt factor   [7]

The net seal opening (separating) force is found by integrating the pressure profile across the sealing face.

$$F_n = WL\ \Delta P\left(\frac{\beta}{\beta + 1}\right) \quad\quad [8]$$

where

$$\beta = \frac{h_1}{h_2}$$

(See Fig. 3 for an illustration of the symbol usuage.)

Thus, the load factor is

$$\overline{F} = \frac{F_n}{A_{SD}\ \Delta P} = \frac{\beta}{\beta + 1} \quad\quad [9]$$

Where

Note for parallel surfaces, $\beta = 1$

$$\overline{F} = 0.50$$

(b) Converging faces, $\beta = 2$

$$\overline{F} = 0.67$$

(c) Diverging faces, $\beta = 1/2$

$$\overline{F} = 0.33$$

The practical range of load factors appears to vary from 0.6 to 0.9 for liquid face seals currently used.

Gas Film Seals

A. Parallel Sealing Surfaces

For gases under conditions of compressible viscous subsonic flow, the pressure profile for parallel films is expressed as (8).

$$P = P_1 \sqrt{1 - \left(1 - \frac{P_2^2}{P_1^2}\right) \frac{x}{L}} \qquad [10]$$

Thus,

$$F_n = \frac{2P_1\left[1 - \left(\frac{P_2}{P_3}\right)^3\right]}{\left[1 - \left(\frac{P_2}{P_1}\right)^2\right]} - P_2 \qquad [11]$$

By algebraic manipulation, it can be shown that the load factor,

$$\overline{F} = \frac{F_n}{A_{SD}\,\Delta P} = \frac{1}{3}\left[1 + \frac{1}{1 + \frac{P_2}{P_1}}\right] \qquad [12]$$

(This formula is identical to the balance modulus presented in (9) and the flow coefficient derived for shaft riding seals found in (5).)

Note that for pressure ratios close to one the gas should behave similar to an incompressible fluid. This is the case since the load factor is 0.5. At very large pressure ratios

$$\overline{F} = \lim_{P_2/P_1 \to 0} \left\{ \frac{1}{3} \left[1 + \frac{1}{1 + \frac{P_2}{P_1}} \right] \right\} = \frac{2}{3} \qquad [13]$$

This high pressure limiting situation is not physically correct, however. In reality, the governing equations break down in that fluid inertia forces become important and the phenomenon of fluid choking can occur. This will be discussed in a section to follow.

Equation [12] is shown plotted in Fig. 4 and illustrates the strong variation of the load factor with pressure ratio. Since $\overline{F} = \overline{F}(P_2/P_1)$, $\overline{F}$ can equal the geometric balance ratio only at one operating condition. This illustrates why it is impossible to completely balance a face seal for all sealed pressure situations and that a slight unbalance at large pressure differentials will greatly overload the seal.

Since Eq. [10] also describes the pressure profile for laminar and fully developed turbulent flows, the load factor predicted by Eq. [13] applies to turbulent flow as well. Note Eq. [13] is independent of film thickness and fluid properties.

B. Sealing Surfaces Represented by Small Linear Tilts

The pressure profile for sealing surfaces undergoing small linear tilts and operating in the compressible viscous flow regime is (8)

$$P = P_1\left[1 + \frac{\left[\left(\dfrac{P_2}{P_1}\right)^2 - 1\right]h_2^2 x(2h_1 + \alpha x)}{2Lh_m\left(h_1 + \alpha x\right)^2}\right] \qquad [14]$$

The load factor can be found by integrating Eq. [14]. The result is after letting $\beta = h_1/h_2$, and $\lambda = P_2/P_1$.

For $\beta > 1$

$$\overline{F} = \frac{\beta}{\beta - 1} - \frac{\beta\sqrt{1 - \lambda^2}}{(1 - \lambda)(\beta - 1)\sqrt{\beta^2 - 1}} \cos^{-1}\left(\frac{1 + \beta\lambda}{\beta + \lambda}\right) \qquad [15]$$

For $\beta < 1$, two cases are considered since this change in the function avoids imaginary terms.

Case I

$\beta^2 - \lambda^2 > 0$:

$$\overline{F} = \frac{-\beta}{1 - \beta}\left\{1 + \frac{1}{1 - \lambda}\sqrt{\frac{1 - \lambda^2}{1 - \beta^2}}\left[\cosh^{-1}\left(\beta\sqrt{\frac{1 - \lambda^2}{\beta^2 - \lambda^2}}\right) - \cosh^{-1}\left(\sqrt{\frac{1 - \lambda^2}{\beta^2 - \lambda^2}}\right)\right]\right\} \qquad [16]$$

Case II

$\beta^2 - \lambda^2 < 0$:

$$\overline{F} = \frac{-\beta}{1 - \beta}\left\{1 + \frac{1}{1 - \lambda}\sqrt{\frac{1 - \lambda^2}{1 - \beta^2}}\left[\sinh^{-1}\left(\beta\sqrt{\frac{1 - \lambda^2}{\lambda^2 - \beta^2}}\right) - \sinh^{-1}\left(\sqrt{\frac{1 - \lambda^2}{\lambda^2 - \beta^2}}\right)\right]\right\} \qquad [17]$$

Note when $\beta = 1$, the result is the parallel film case which is described by Eq. [13]. Eqs. [15], [16] and [17] are presented in (9). (However, in (9) the argument of the arccosine in Eq. [15] has a pressure ratio omitted in the numerator. The plotted results are correct, however, in (9).)

Choked Flow Conditions

For subsonic viscous flows the analyses yield the analytical solutions presented in the previous section. For large pressure ratios and/or relatively small flow length-to-gap ratios, the inertia forces must be accounted for and choked flow will result. Choked flow in seals generally occurs when the physically limiting condition of sonic velocity is reached at the seal exit.

Since inclusion of fluid inertia makes the flow equations nonlinear, the flow is solved using an approximate integrated average model. Also, under choked flow conditions, sufficiently high velocities occur at the entrance that entrance pressure losses are significant.

A. Parallel Sealing Surfaces

The analysis is described in detail in (7). It is separated into two parts, which are considered separately and then matched. One part is an analysis of the entrance flow, while the other part is an analysis of the seal leakage path itself. The governing conservation equations are combined through relations to yield a Mach number - mean friction factor relation. The mean friction factor is related to the Reynolds number by the relation

$$\bar{f} = C R_e^{-n} \qquad [18]$$

Where the values for the coefficient C and exponent n depend on the flow regime as discussed in (8). Once the Mach number at any flow length distance x, is found from the relation

$$\frac{4\bar{f}x}{D} = \left[\frac{1}{\gamma} \left\{ \frac{1 - M_1^2}{M_1^2} - \frac{1 - M_x^2}{M_x^2} \right\} + \frac{\gamma + 1}{2\gamma} \left\{ \ln \frac{\frac{\gamma + 1}{2} M_1^2}{1 + \frac{\gamma - 1}{2} M_1^2} - \ln \frac{\frac{\gamma + 1}{\gamma} M_x^2}{1 + \frac{\gamma - 1}{2} M_x^2} \right\} \right]$$

[19]

The pressure distribution can be found from

$$P_x = \frac{P_1 M_1}{M_x} \sqrt{\frac{1 + \frac{\gamma - 1}{2} M_1^2}{1 + \frac{\gamma - 1}{2} M_x^2}}$$

[20]

Then the load factor is found from

$$\bar{F} = \frac{\int_0^L P_x \, dx}{A_{SD} \, \Delta P}$$

[21]

The integral in Eq. [21] is evaluated numerically in (7) by using Simpson's rule.

B. Sealing Surfaces Represented by Small Linear Tilts

When the sealing surfaces are deformed, the area change complicates the equation relating the mean friction factor and Mach number squared. The equation that must be solved is

$$\frac{dM^2}{dx} = \frac{2M^2\left(1 + \frac{\gamma - 1}{2} M^2\right)}{h(1 - M^2)} \left\{ \gamma M^2 \overline{f}(x) - \frac{[h + x \sin \alpha]}{x} \right\} \qquad [22]$$

This equation must be solved numerically. The Runge-Kutta solution technique used is described in (10). Again, once the Mach number distribution is known, the pressure distribution can be found from

$$P_x = \frac{P_1 A_1}{A_x} \frac{M_1}{M_x} \sqrt{\frac{1 + \frac{\gamma - 1}{2} M_1^2}{1 + \frac{\gamma - 1}{2} M_x^2}} \qquad [23]$$

The load factor is again evaluated in (10) by evaluating Eq. [21] numerically using Simpson's rule.

RESULTS AND DISCUSSION

Results will be obtained utilizing the various solutions representative of both subsonic and choked flow conditions. The first case has already been considered (i.e., subsonic flow between parallel sealing surfaces). As previously described, Fig. 4 shows the load factor variation with pressure ratio varying from one through 10. Figure 5 extends the load factor variation to pressure ratios of 1000 for parallel sealing surfaces. Both isentropic entrance conditions and conditions representative of an entrance loss coefficient of 0.6 are considered. Note for the isentropic entrance condition case, the flow is choked for a pressure ratio of ten and the flow is probably turbulent when the pressure ratio has exceeded 50. This case

illustrates that a maximum limiting value of about 70.5 is reached for ultra high pressure ratios. The results in Fig. 5 were obtained with the film thickness fixed at 0.0002 in. This film thickness is found to be representative of gas film seal operation (4). Also shown plotted in Fig. 5 is Eq. [12], which is the classical subsonic flow equation which, although not applicable in a strict sense, shows that a limiting value of 0.67 is predicted. However, if a 0.6 entrance loss is accounted for (which may be the case in real seal applications (8)), Fig. 5 shows that a maximum value (0.645) is achieved for choked flow, then the load factor actually decreases slightly with pressure over the entire range studied. Thus, as anticipated, since the fluid physics is different for choked flow, the behavior of the load factor differs greatly than for subsonic flow conditions.

Figure 6 presents the load factor variation with pressure ratio for both linearly diverging and converging sealing faces. Beta ($=h_1/h_2$) is the parameter that is varied in this study as the pressure ratio is varied from one-tenth to ten. Beta equal to one represents the parallel sealing surface reference case. This figure also shows that the numerical solution (10) agrees with the analytical solutions Eqs. [15], [16], and [17]. This figure illustrates the deviation of the load factor with pressure ratio which can be applied to evaluate the magnitude of the induced lifting force or contacting forces due to coning of the seal face. As expected, the larger the deformation, the more the deviation from the parallel sealing surface case. If

thermal coning should be present in a gas film seal, Fig. 6 can be used to predict the resulting increase in seal face loading which would be detrimental to the seal operation. On the contrary, if the application permits using a converging tapered face, this figure can be used to estimate the degree of added or increased separating force that may be generated.

For subsonic flow conditions, it was seen that the load factor is independent of mean film thickness. Under choked flow conditions, the load factor does depend on film thickness but not strongly over a practical range of film thicknesses. This is illustrated in Fig. 7. The film thickness is varied from 50 to 500 microinches. A family of curves is shown for sealed pressure ratios of 10, 50, 100, 1000, and 10000. The entrance flow conditions were assumed to be isentropic.

Figure 8 essentially repeats Fig. 7 except the entrance flow was assumed to behave as a flow with a 0.6 entrance loss coefficient. By comparing Fig. 8 with Fig. 7, it is seen that this case more strongly depends on the mean film thickness. This dependence, of course, is especially important for noncontacting operation which will usually be the mode of operation for high pressure differential sealing.

Figure 9 shows the load factor-film thickness variation for choked flow and a one milliradian tilted seal face (divergent). For high pressure operation the tilt angle is a more meaningful parameter rather than the inlet-to-exit film thickness ratio, β. It can be shown that

$$\alpha = \frac{2h_m(1 - \beta)}{\Delta R(1 + \beta)}$$

Alpha values of one and two milliradians are representative of face deformations that can occur in gas film seals. Generally alpha values are so small that they are virtually impossible to measure but can be found from stress analyses of the seal ring. Figure 9 also illustrates the various flow regimes that the seal can encounter.

Figure 10 shows the corresponding negative one-milliradian face deformation case (converging face). Note the lesser sensitivity to film thickness than the divergent face case.

The load factor variation for relatively large tilted surfaces of positive and negative two milliradian and a pressure ratio of ten is shown in Fig. 11. Note the extreme sensitivity of load factor on the mean film thickness, indicating an extremely high face loading if a means of achieving positive surface separation is not provided.

Pressure Balancing With Hydrodynamic Forces Present

For gas film seals operating under severe conditions, e.g., high pressure ratios, operation under conditions with rubbing contact may be virtually intolerable due to high face loading. Thus, hydrodynamic lift devices such as self-acting lift pads (11) must be incorporated into the primary seal face design. The seal force balance should now take into account this additional force.

In some applications such as aircraft gas turbine seals, the sealed pressure ratio depends on such factors as the mode of operation, e.g.,

takeoff, climb, cruise and ambient pressure which varies with altitude. Unfortunately, the geometric balance ratio, η, is of necessity fixed for a particular design. Thus, a suitable secondary seal diameter must be chosen which will enable satisfactory operation over a wide range of conditions.

Table 2 shows a comparison between the geometric balance ratio and the load factor for the NASA self-acting lift pad seal. (The operating film thickness effect on the load factor is accounted for.) The geometric balance ratio is, of course, constant for all design points. However, the load factor varies (see table 2). And this is because of the different pressure profile shapes for each design point. Note that the net closing force due to the hydrostatic pressure is small (4.7 to 2.0 lbf) at the four design points. Thus, the self-acting pads act, principally, against the spring force in this particular design. This is the design philosophy used for the NASA self-acting lift pad design. The philosophy could vary with application.

As previously mentioned in a conventional seal, the net closing force is resisted by solid-surface rubbing contact; thus, a total force balance is achieved. But in self-acting seals the force balance is achieved without rubbing contact. Therefore, for a given design point, the seal will operate at a film thickness such that the total opening force exactly balances the total closing force. This operating film thickness is obtained by plotting total opening forces and total closing forces as a function of film thickness. The intersection (see Fig. 12) of these curves is the steady state equilibrium (operating) film thickness.

The incorporation of self-acting lift pads can be viewed as a means of noncontact operation of a gas film seal under a wide range of conditions. These conditions would yield face loadings that are too high for ordinary gas film seals. The conditions could be due to pressure, face distortion or entrance conditions. Figure 5 shows that entrance conditions can have a marked effect on the load factor. Since entrance conditions can vary for given designs, the lift pad forces can be designed to accommodate for these variations. Thus for high pressure gas sealing applications, incorporation of lift pads are not only important for high axial film stiffness for dynamic tracking, but also for maintaining positive film separation.

CONCLUDING REMARKS

An analytical study of pressure balancing in gas film seals was conducted. Both subsonic and choked flow conditions, parallel and deformed seal surfaces represented by small linear tilts were investigated. Analytical predictors for the load factor in the compressible viscous, subsonic flow regime are presented. Conditions of seal operation under choked flow were investigated by utilizing numerical solutions. The following pertinent results were found.

1. For classical viscous subsonic flow, the load factor is a strong function of sealed pressure ratio and increases with pressure ratio but is independent of film thickness. This is true for both laminar and fully developed turbulent flow.

2. For choked flow the load factor depends not only on pressure ratio, but also on film thickness, entrance conditions, and flow regime.

a. For isentropic entrance conditions, the load factor reaches a limiting value of approximately 0.70 at pressure ratios greater than 50. The flow is turbulent for these conditions.

b. For seal flows with a 0.6 entrance loss coefficient, a maximum of approximately 0.64 was reached; then the value began to drop fairly rapidly until the pressure ratio exceeded 40 where turbulence was set to occur. The load factor then decreased relatively slowly.

3. The film thickness was varied from 0.00005 in. to 0.0005 in. for conditions representative of gas film seal operation. Results indicate that for pressure ratios greater than 5, the load factor was sensitive to film thickness for a fixed pressure ratio. Also the same study with 0.6 entrance loss conditions showed film thickness sensitivity but differed greatly from the isentropic entrance condition case.

4. The effects of linear tilts representing convergent and divergently deformed faces indicated the importance of controlling and accounting for seal face deformations.

5. Load factor variations due to high pressures, distortions, entrance effects, etc. can be accommodated by incorporating self-acting lift pads to the seal face. This is especially true for multi-point operation. The hydrodynamic force generated by the lift pads is shown to keep the seal "balanced" even though the secondary seal diameter is fixed.

REFERENCES

1. Anon., "Dynamic Sealing: Theory and Practice," Koppers Company, Inc., Baltimore, Md.

2. Mayer, E. (B.S. Nau, trans.), "Mechanical Seals," American Elsevier, 1970.

3. Pape, J. G., "Fundamental Aspects of Radial-Face Seals," Technische Hogeschool, Delft, Netherlands, Rep. WTHD-17, Dec. 1969.

4. Burcham, R. E., "Liquid Rocket Engine Turbopump Rotating Shaft Seals," NASA proposed Special Publication.

5. Schweiger, F. A., "The Performance of Jet Engine Contact Seals," Lubr. Eng., 19, 232-238 (1963).

6. Slayton, R., Thomas, R. L., and Parks, A. J., "Development of Mainshaft Seals for Advanced Airbreathing Propulsion Systems," Semiannual Report No. 1, Contract NAS3-7609, January 20, 1966.

7. Zuk, J., and Smith, P. J., "Quasi-One-Dimensional Compressible Flow Across Face Seals and Narrow Slots. II - Computer Program," NASA TN D-6787, 1972.

8. Zuk, J.: Fundamentals of Fluid Sealing, ASLE course notes on Fluid Sealing (also NASA TNE-6910).

9. Stein, P. C., "A Discussion of the Theory of Sealing Devices," presented at the Southern New England Section, Society of Automotive Engineers, Hartford, Conn., Mar. 7, 1961. (Available from the Stein Seal Company, Philadelphia, Pa., 19132.)

10. Zuk, J., and Smith, P. J., "Computer Program for Quasi-One-Dimensional Compressible Flow with Area Change and Friction - Application to Seals," Proposed NASA Technical Note.

11. Ludwig, L. P., Zuk, J., and Johnson, R. L., "Design Study of Shaft Face Seal with Self-Acting Lift Augmentation IV - Force Balance," NASA TN D-6568, 1972.

Table 1 - Other names used for the geometric balance ratio or

modulus and pressure profile load factor that are found in the

literature

I. Geometric balance ratio or modulus $= \dfrac{\text{hydrostatic pressure closing area}}{\text{sealing dam face area}}$	
Name	Reference
Area ratio	(2)
Balance factor[*] (used by some seal manufacturers)	(3)
Pressure balance ratio (modulus)	(4)
Geometric unbalance ratio	

II. Pressure profile load factor $\overline{F} = \dfrac{\text{sealed pressure force}}{\text{sealed pressure opening force}}$ or $\quad$ Pressure profile factor $= \dfrac{\text{net or ave seal face pressure}}{\text{sealed pressure differential}}$	
Name	Reference
Balancing modulus	(4)
Flow coefficient	(5)
Load Ratio	(3)
Pressure form factor	(6)
Dimensionless force	(7)

[*]Pape (3) also defined a complement to unity which is called the degree
of balance.

Table 2 - Seal force balance indicators for

several design conditions

Design point (represents aircraft engine operating mode)	Geometric balance ratio	Pressure profile load factor	Net closing due due to hydrostatic pressure,[a] lbf
1 - Idle	0.70	0.61	4.7
2 - Cruise		.68	3.0
3 - Takeoff		.69	2.0
4 - Climb		.68	4.5

[a]Pneumatic closing force minus opening force.

$P_0 > P_3$

PRIMARY SEALING FACE

SEAL OPENING FORCE

(SEALING DAM)

P_3

P_2

SPRING

NOISEPIECE (SEAL RING)

HOUSING

P_1

PISTON RING SECONDARY SEAL

P_0

HYDROSTATIC CLOSING FORCE

P_0

SEAL SEAT

SHAFT

SECONDARY SEAL DIAMETER
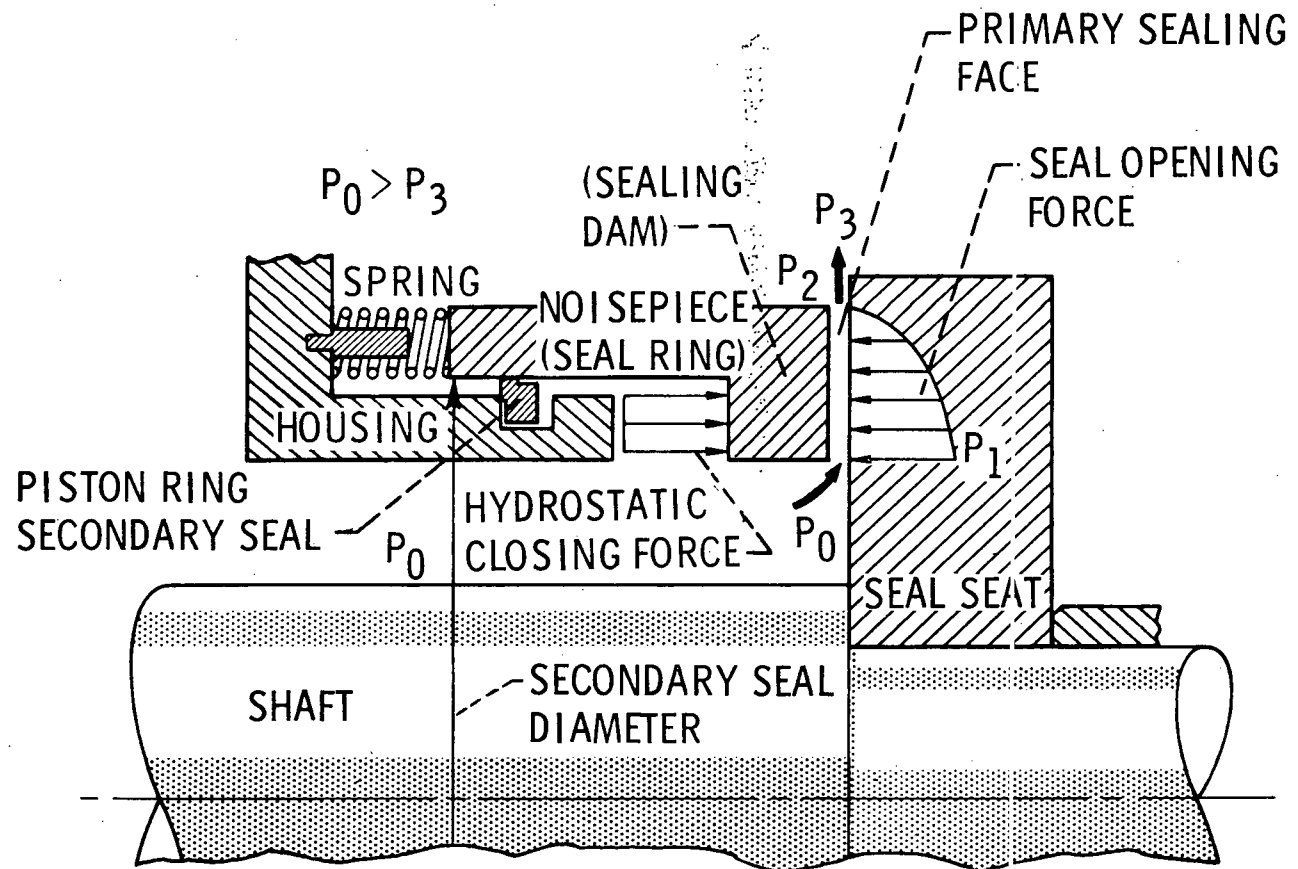
CS-66529

Figure 1. - Pressure-balanced face seal.
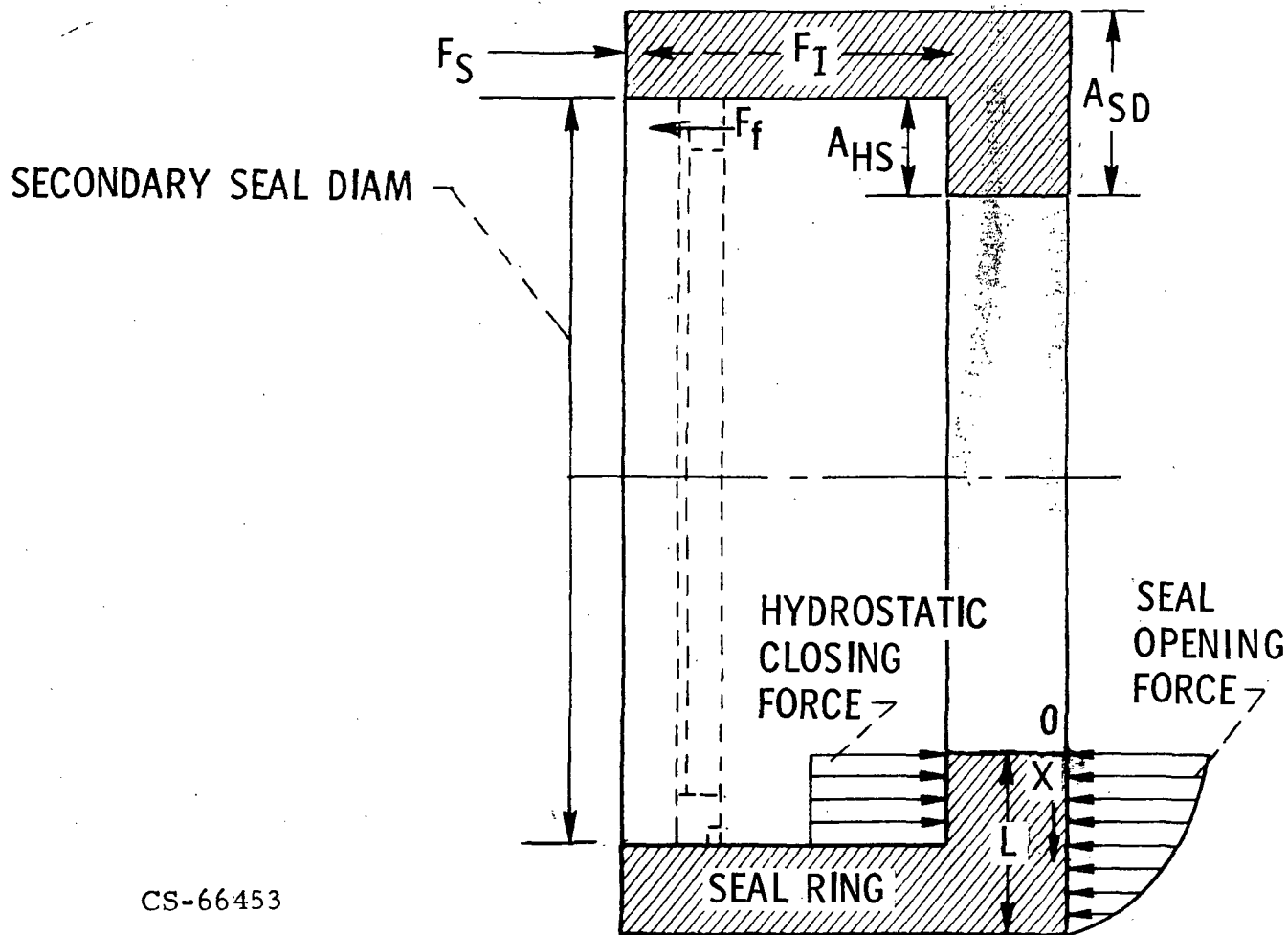
Figure 2. - Schematic of radial face seal identifying the nomenclature.

CS-66453
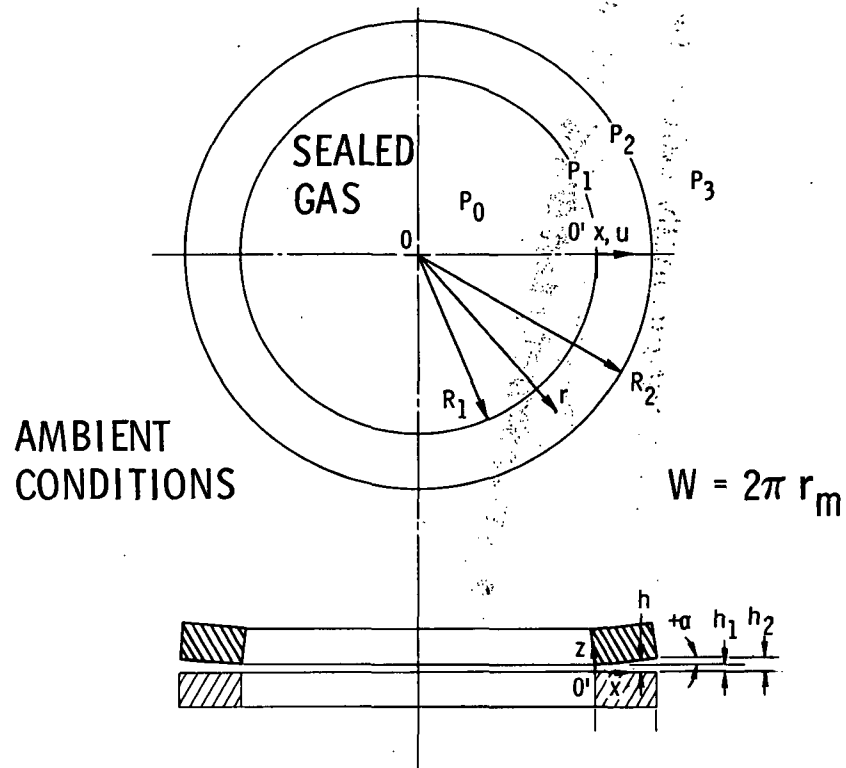
Figure 3. - Model of the primary sealing faces (Dam) with
a small tilt angle (not to scale). Diverging face shown.
(Upper ring removed for clarity in top view.)

CS-66434

$$\overline{F} = \frac{1}{3}\left(1 + \cfrac{1}{1 + \cfrac{P_2}{P_1}}\right)$$
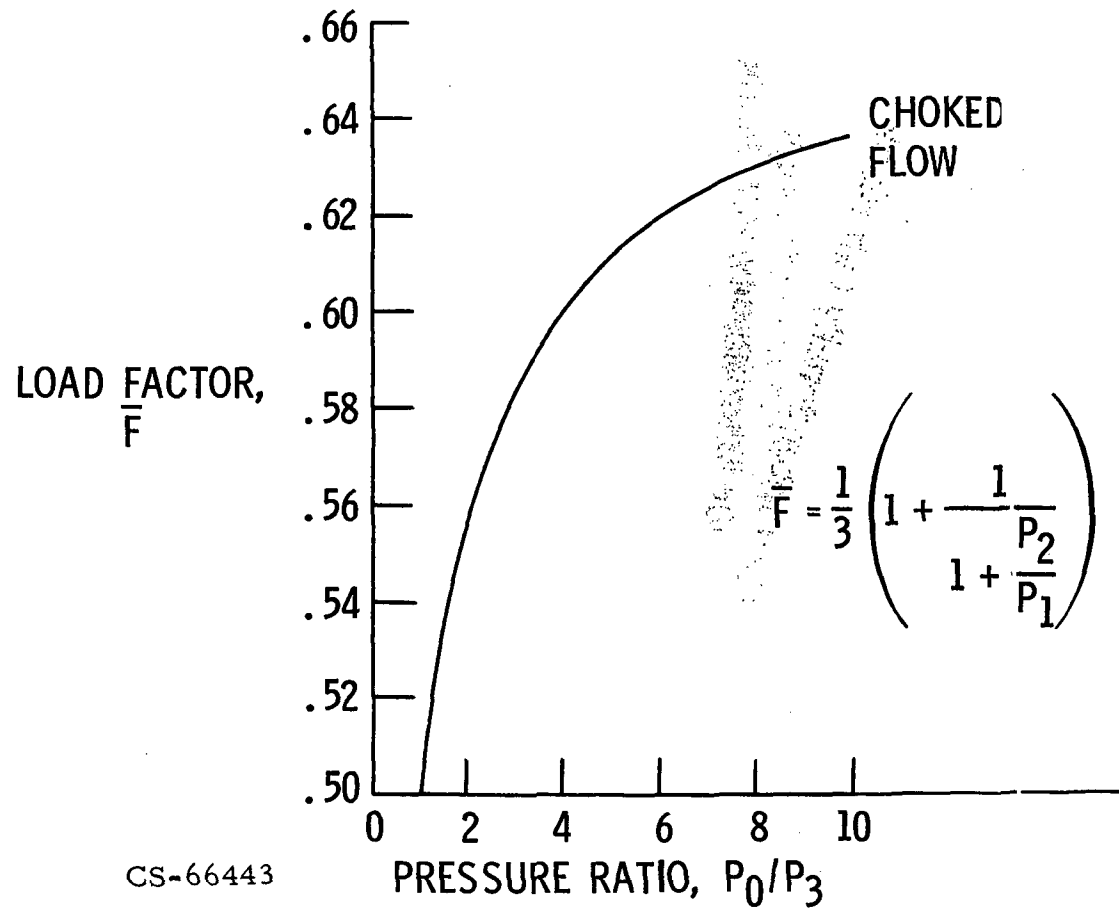
Figure 4. - Load factor variation with pressure ratio in the subsonic flow regime, parallel sealing surfaces.
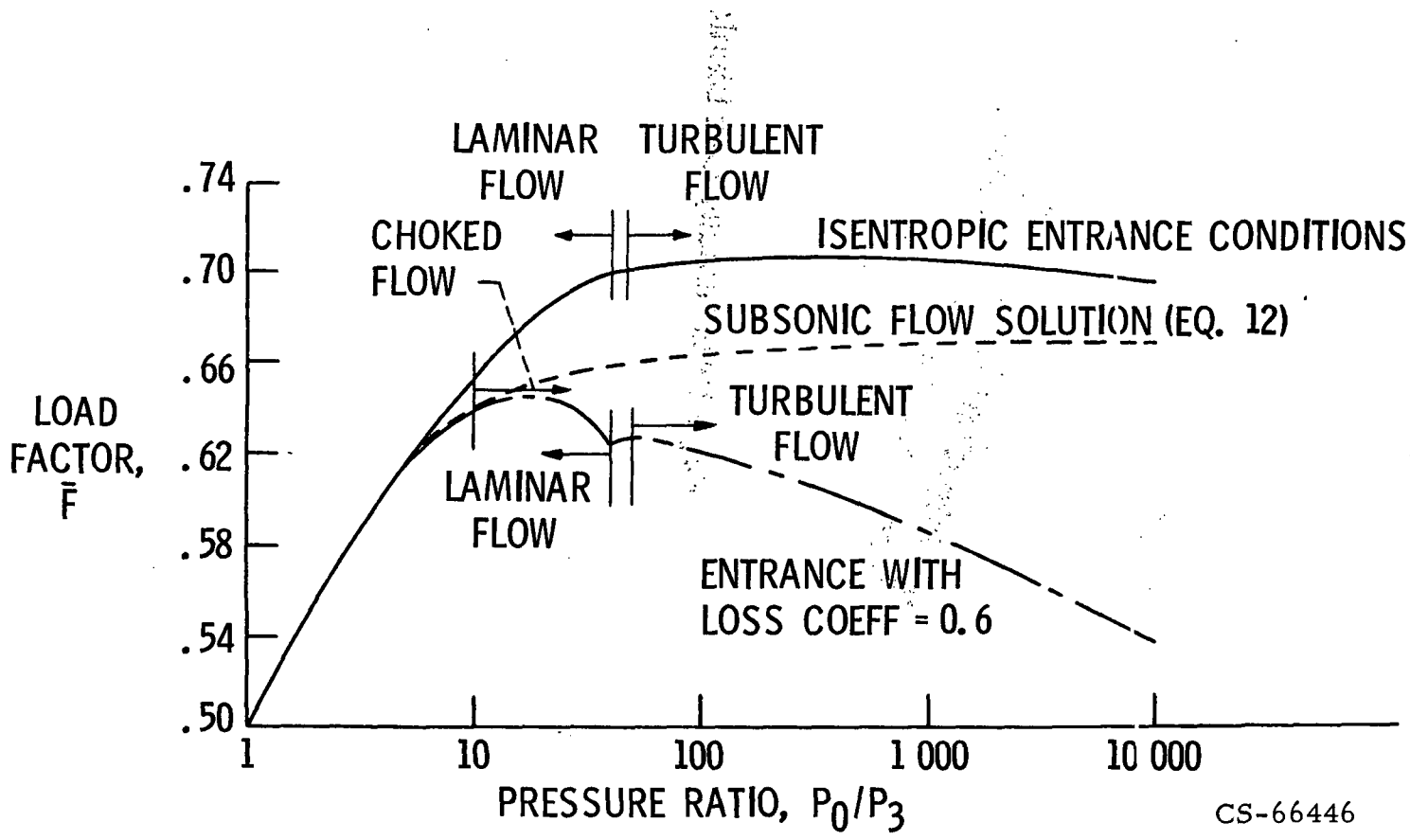
CS-66443

Figure 5. – Load factor variation with pressure ratio over a wide range of conditions, parallel surfaces with a mean film thickness of 0. 2 mil.
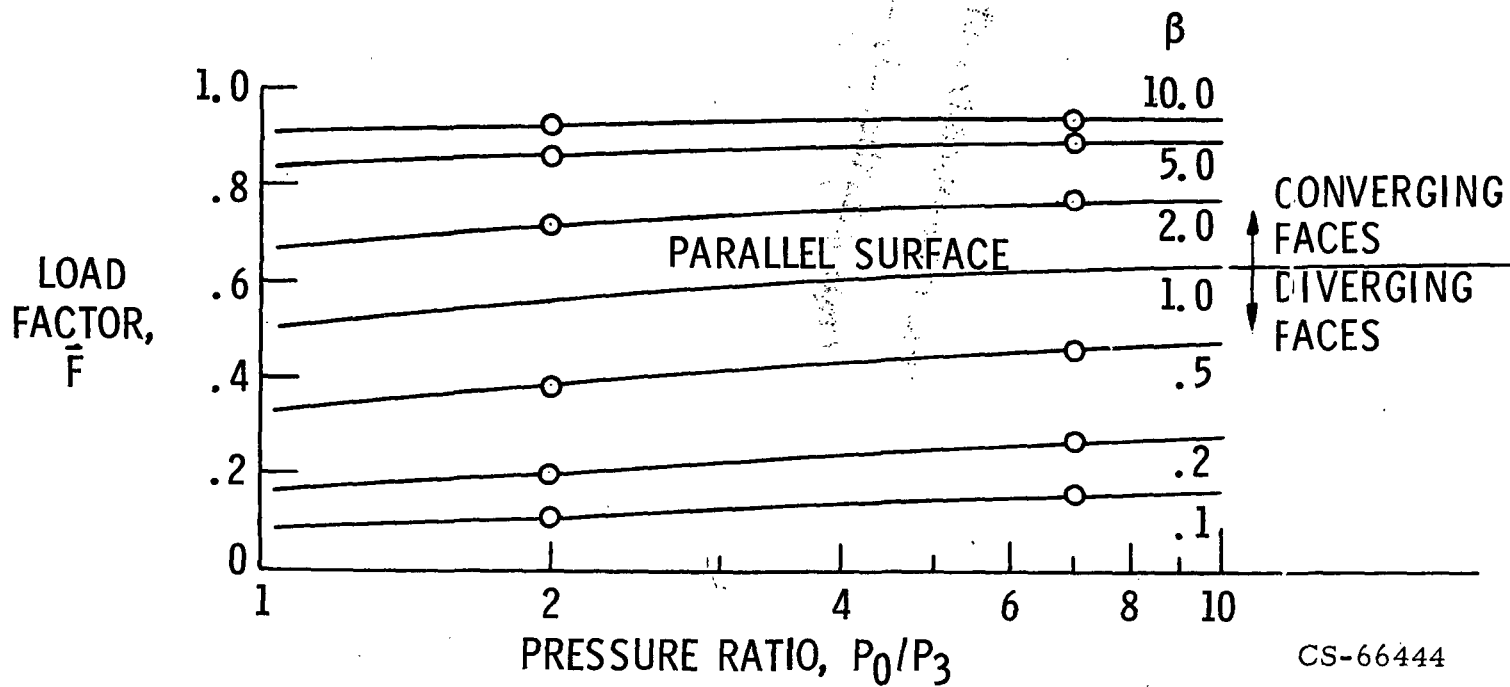
Figure 6. – Load factor variation with pressure ratio for subsonic flow.
Both linearly converging and diverging sealing surfaces are shown.
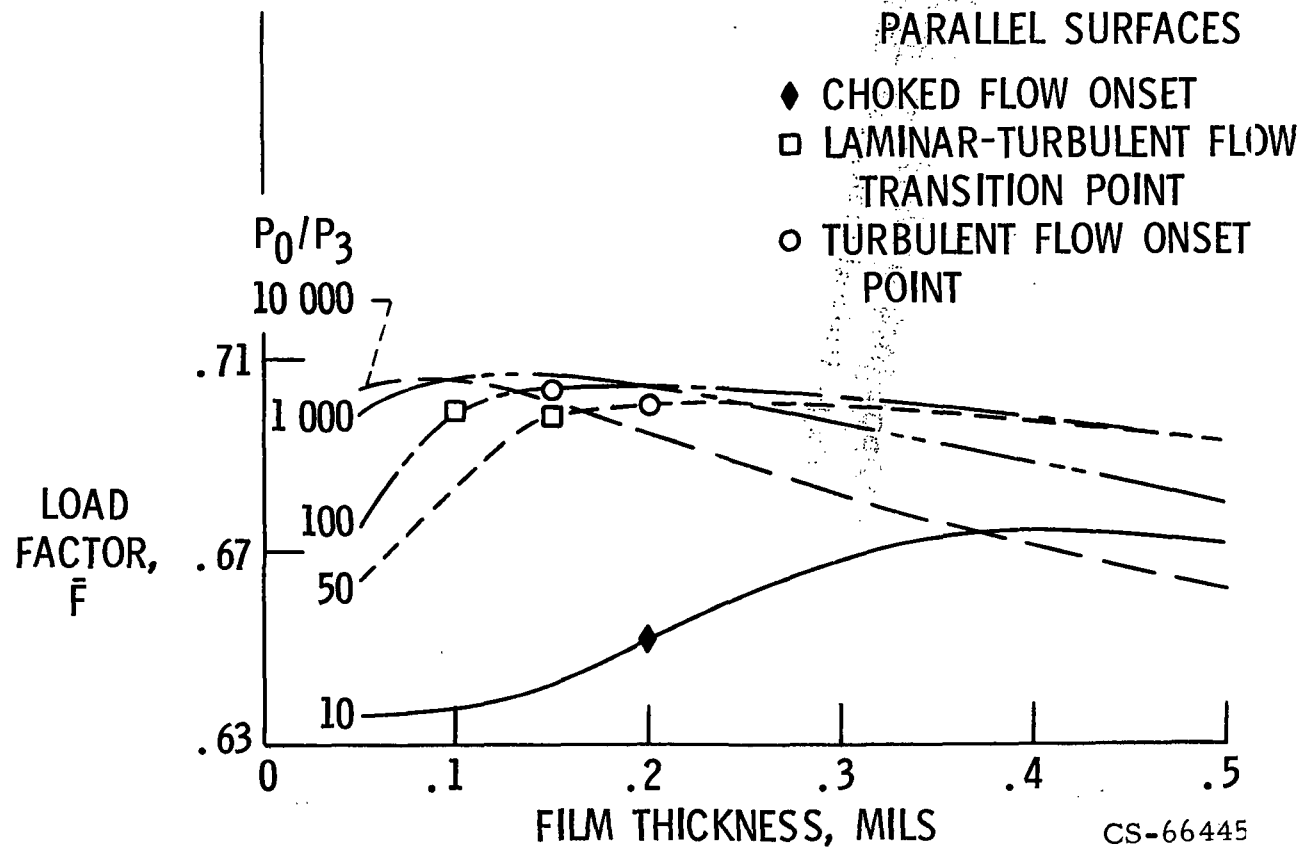
Figure 7. - Load factor variation with film thickness for
several pressure ratios, parallel sealing surfaces,
isentropic entrance flow conditions.
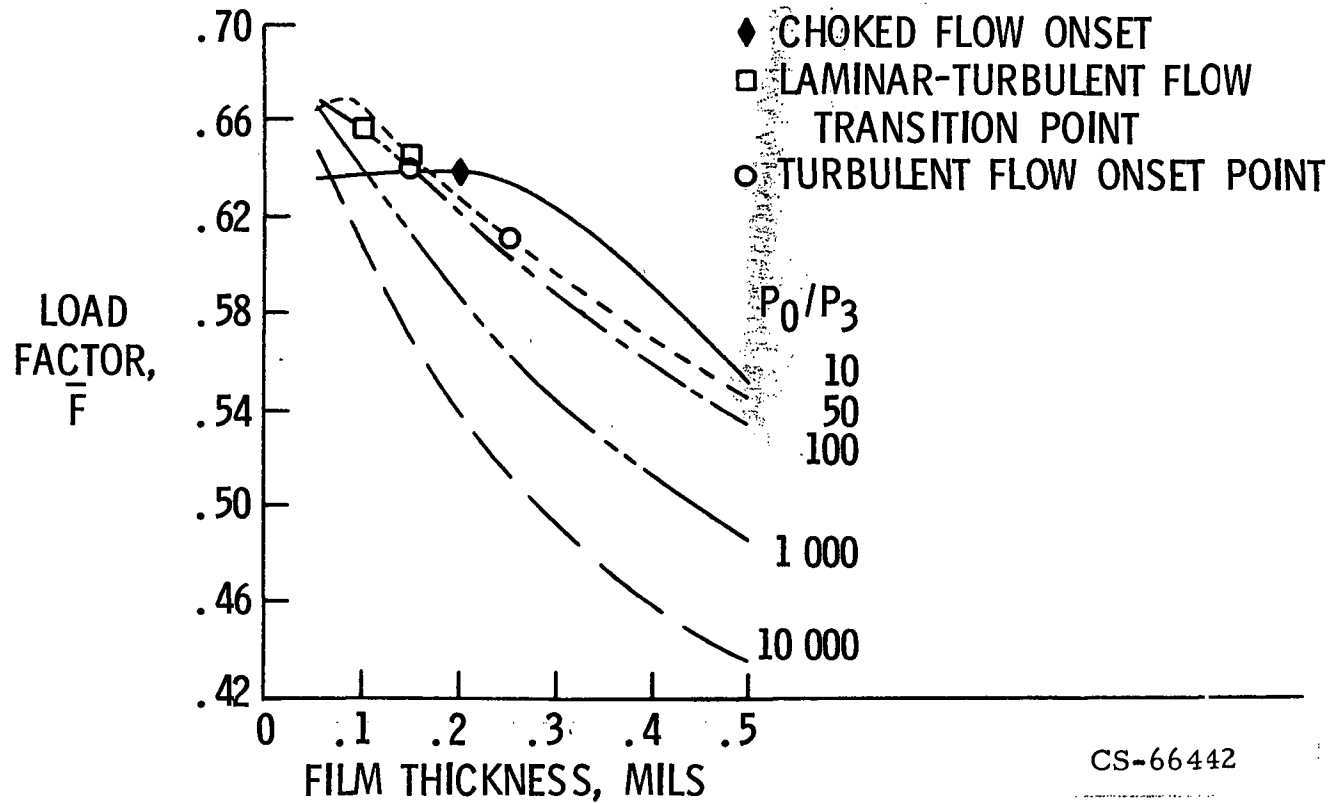
Figure 8. - Load factor variation with film thickness for several pressure ratios, parallel sealing surfaces, entrance flow represented by a 0. 6 entrance loss condition.
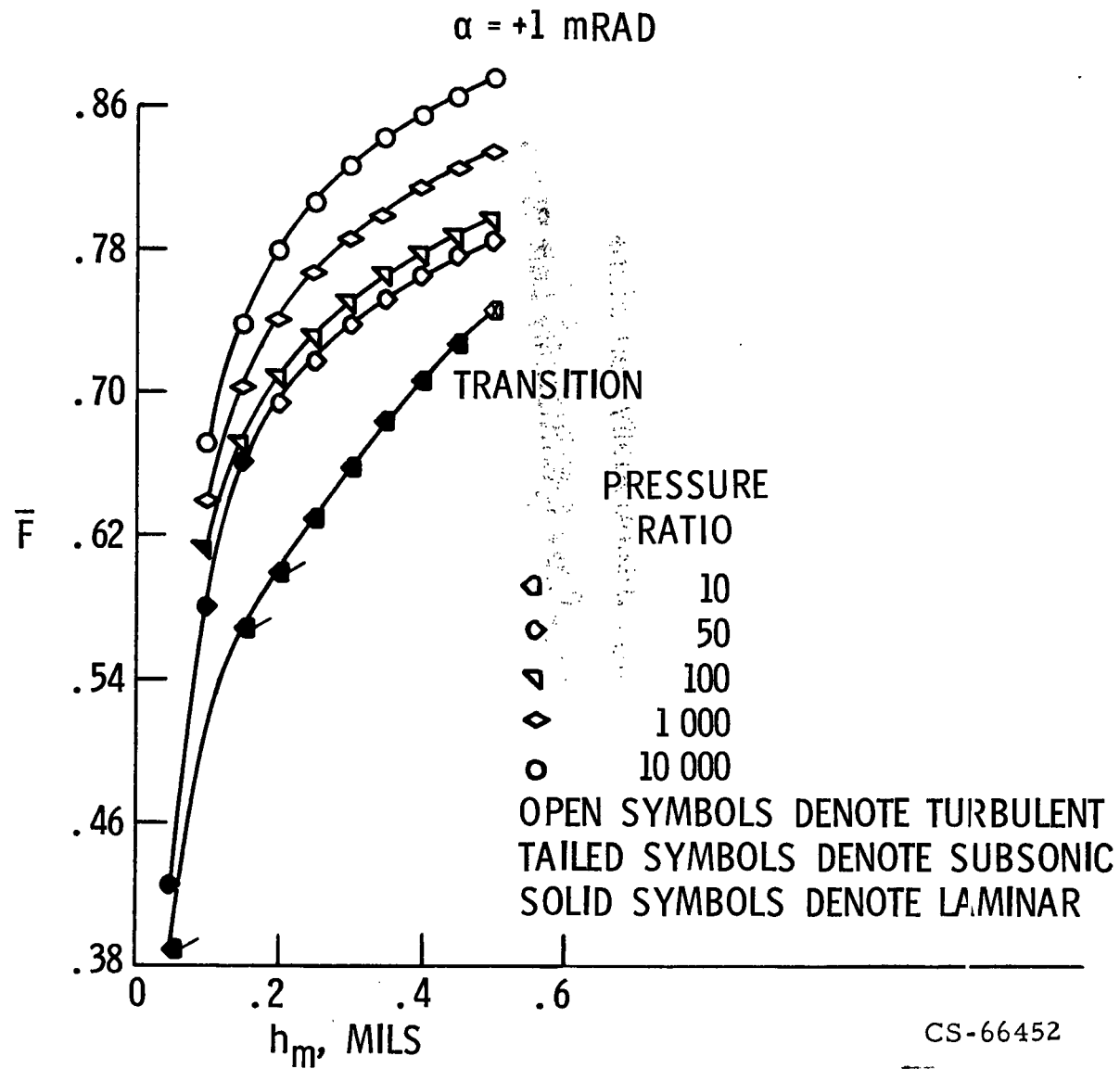
Figure 9. – Load factor variation with film thickness for several pressure ratios, linearly tilted sealing surfaces of positive one milliradian (divergent).

$\alpha = -1$ mRAD

PRESSURE
RATIO

▷   10
◇   50
◁   100
◁   1 000
□   10 000

OPEN SYMBOLS DENOTE TURBULENT
TAILED SYMBOLS DENOTE SUBSONIC
SOLID SYMBOLS DENOTE LAMINAR
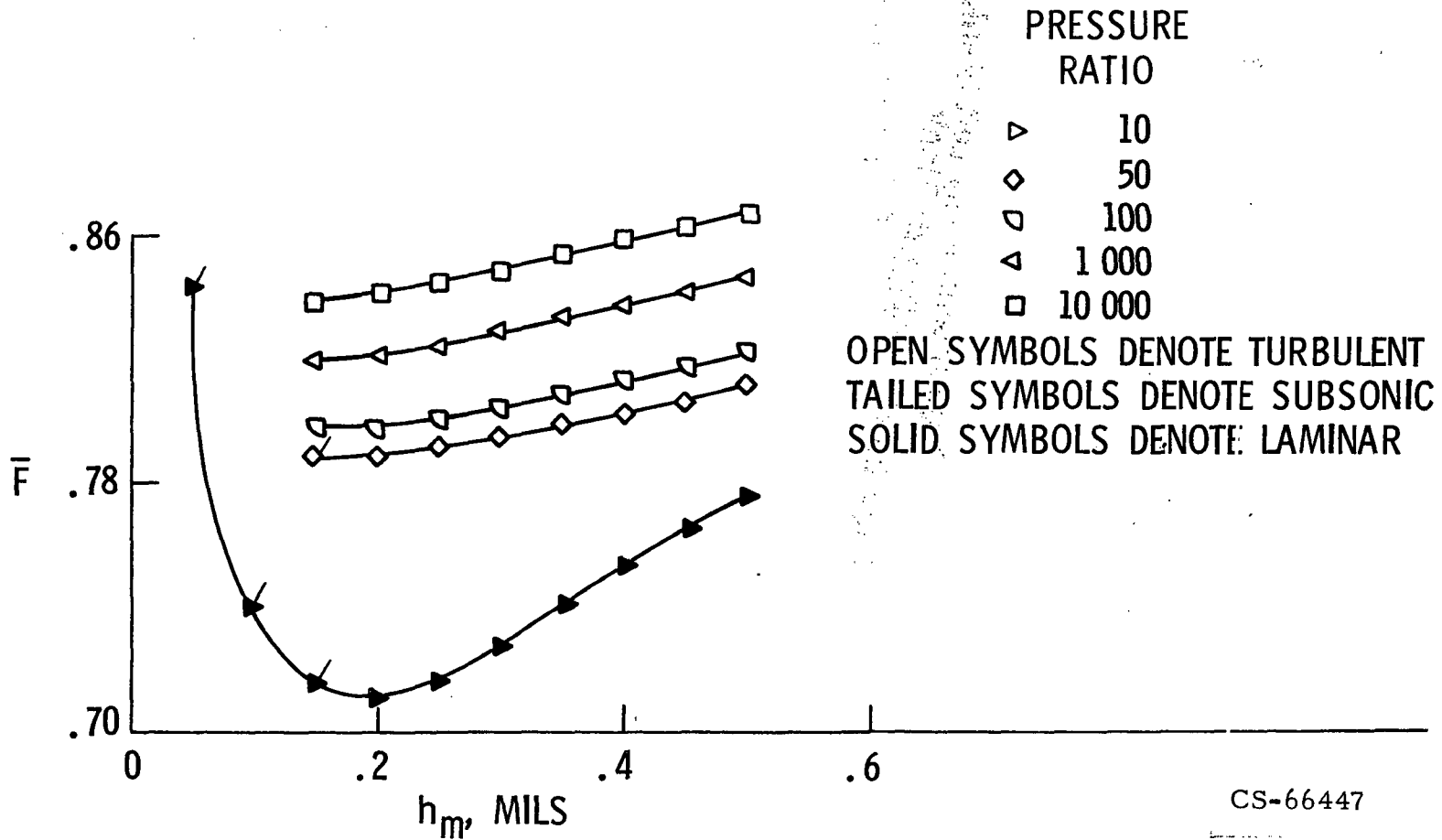
CS-66447

Figure 10. - Load factor variation with film thickness for several pressure ratios,
linearly tilted sealing surfaces of negative one milliradian (convergent).
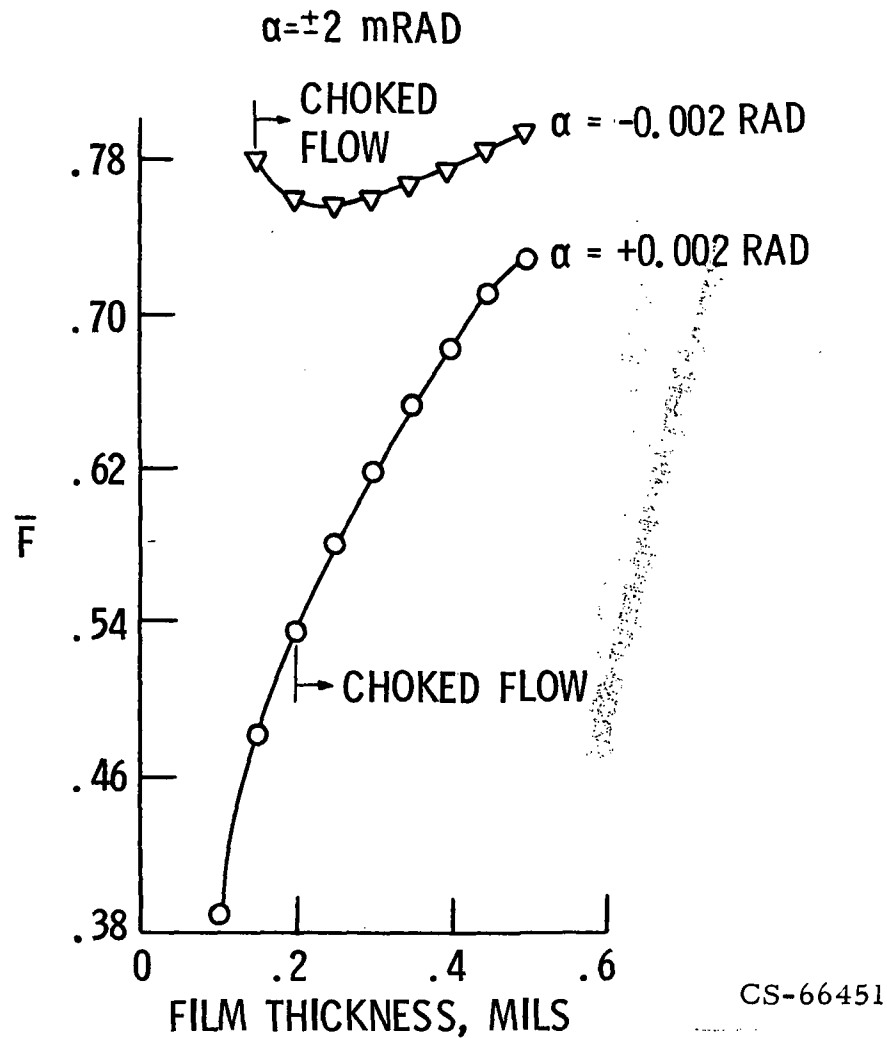
Figure 11. - Load factor variation with film thickness for positively and negatively tilted surfaces of two milliradians and a pressure ratio of 10.
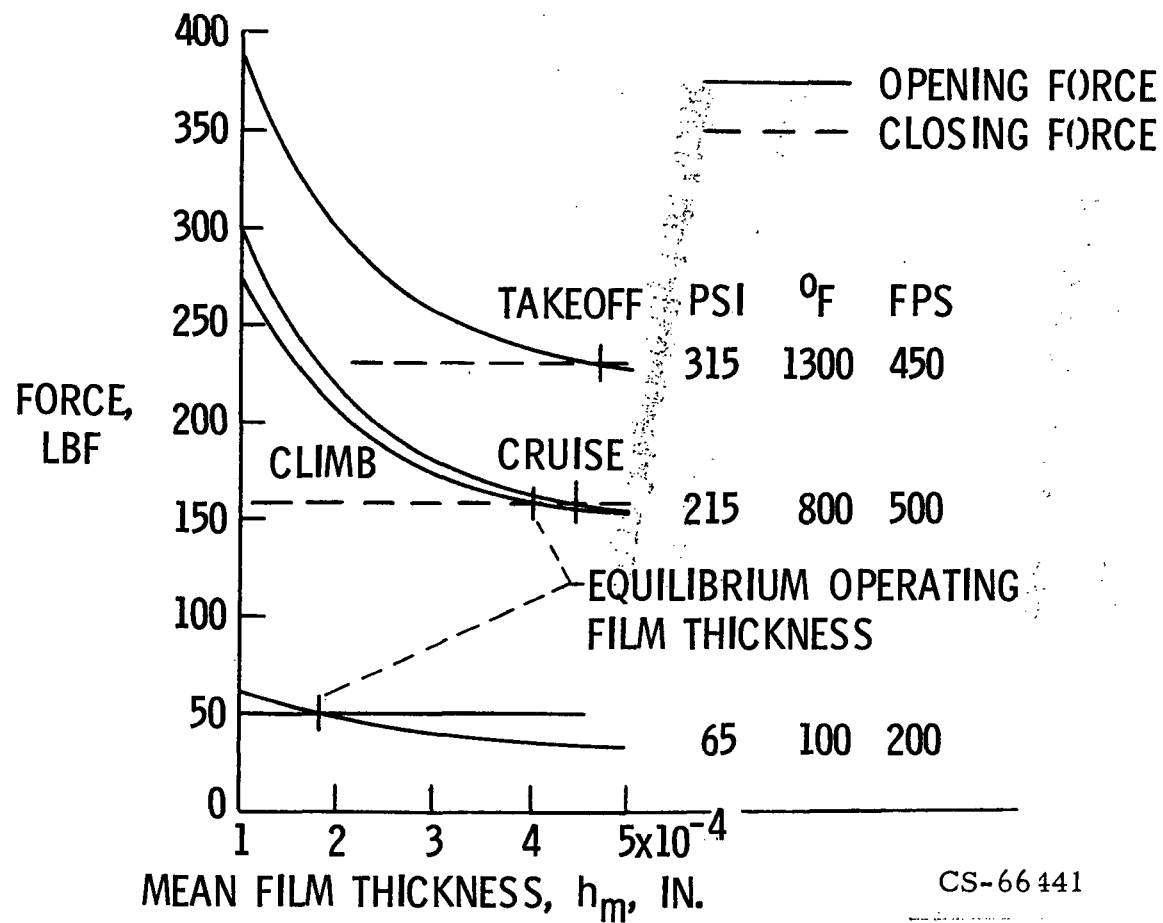
Figure 12. - Equilibrium gas film thickness as determined by total seal opening and closing forces, parallel surfaces (11).